

## Interfacial reactions and surface analysis of W thin film on 6H-SiC

**T.T. Thabethe<sup>a\*</sup>, T.T. Hlatshwayo<sup>a</sup>, E.G Njoroge<sup>a</sup>, T. G. Nyawo<sup>b</sup>, T. P. Ntsoane<sup>c</sup> and J. B. Malherbe<sup>a</sup>**

*(a) Department of Physics, University of Pretoria, Pretoria, 0002, South Africa*

*(b) Department of Physics, University of Zululand, KwaDlangezwa, 3886, South Africa*

*(c) South African Nuclear Energy Corporation SOC Limited, Pretoria, 0001, South Africa.*

### Abstract

Tungsten (W) thin film was deposited on bulk single crystalline 6H-SiC substrate and annealed in vacuum at temperatures ranging from 700 to 1000 °C for 1 hour. The resulting solid-state reactions, phase composition and surface morphology were investigated by Rutherford backscattering spectroscopy (RBS), grazing incidence X-ray diffraction (GIXRD) and scanning electron microscopy (SEM). XRD was used to identify the phases present and to confirm the RBS results. The RBS spectra were simulated using the RUMP software in order to obtain the deposited layer thickness, composition of reaction zone and detect phase formation at the interface. RBS results showed that interaction between W and SiC started at 850 °C. The XRD analysis showed that WC and CW<sub>3</sub> were the initial phases formed at 700 °C and 800 °C. The concentration of the phases was however, too low to be detected by RBS analysis. At temperatures of 900 °C and 1000 °C, W reacted with the SiC substrate and formed a mixed layer containing a silicide phase (WSi<sub>2</sub>) and a carbide phase (W<sub>2</sub>C). The SEM images of the as-deposited samples showed that the W thin film had a uniform surface with small grains. The W layer became heterogeneous during annealing at higher temperatures as the W granules agglomerated into island clusters at temperatures of 800 °C and higher.

**Keywords:** tungsten, SiC, interface, reactions, annealing

*\*Corresponding author: T. T. Thabethe, Tel: 012 420 4510, email: thabby.theo@gmail.com*

## 1. Introduction

High temperature gas cooled reactors (HTGRs) are considered as an alternative means of electricity generation. In these reactors silicon carbide (SiC) is used as the main diffusion barrier of fission products (FPs) for fuel kernel encapsulation in the tristructural-isotropic (TRISO) particles [1, 2]. The TRISO particle retains most of the FPs quite effectively with the exception of release of silver (Ag) during reactor operating conditions [1]. Intensive investigations have been undertaken to understand the migration behaviour of Ag through SiC [1–7]. However no clear explanation has been given for the silver release. The grain boundary diffusion of silver in SiC was first suggested as the migration mechanism [1] but it has subsequently been ruled out [2, 3, 5].

There had also been reports (see [1] for a summary) on the reactions between some FPs and SiC, raising some concerns on the integrity of SiC as a coating layer [3, 4] and questioning the ability of SiC as the main diffusion barrier to FPs after such reactions. Interaction of palladium (Pd) with SiC has been investigated and was found to enhance the migration of silver [6–9]. The interaction between high yield FP such as zirconium (Zr) and SiC has also been reported [10,11].

Tungsten (W) is one of the preferred ohmic contact metals with SiC for semiconductor device applications due to its splendid chemical, physical and mechanical properties; such as good heat resistance, low resistivity, high thermal conductivity, irradiation resistance, exceptional corrosion and abrasion resistance [12–16]. In HTGRs, W has been considered to play a protective role for SiC, which could be added as one of the layers on the TRISO particle [12,17]. Coating of SiC layer with W will assist in improving the shielding effect, which will allow for high burn up and enrichment without degrading the TRISO particle [2]. Thus, it is very important to understand the structural composition, thermal stability, interface reactions, and inter-diffusion behaviour between the W and SiC under varying thermal conditions.

Previous studies have shown that at the W-SiC interface, reaction and inter-diffusion take place leading to the formation of silicides and carbides [13, 18]. Son *et al.* [12] investigated the joining effect of W-SiC (bulk W film) by hot pressing SiC powder (of 30 nm particle size) with tungsten powder (average particle size 0.6  $\mu\text{m}$ ) at 1700–1900  $^{\circ}\text{C}$  for 10–120 min. They found that the hot pressing of W and SiC resulted in the formation of W silicides ( $\text{WSi}_2$  and  $\text{W}_5\text{Si}_3$ ) and W carbides (WC and  $\text{W}_2\text{C}$ ). Lee *et al.* [19] studied the effect of adding SiC nanowires with W powder to form composites and investigated the interface microstructure

and mechanical properties. The SiC nanowires and W powder were fused by spark plasma sintering process and heated at 1700 °C for 3 min to form composites. W<sub>2</sub>C and W<sub>5</sub>Si<sub>3</sub> phases were formed by the reaction between SiC and W during the sintering process. Reactions in thin films are known to start at lower temperatures as compared to bulk [20]. The reported reaction temperature of W thin film is 700 °C forming silicides [16]. In bulk W-SiC samples, the initial reaction occurs at a temperature of 1200 °C which results in the formation of silicides and carbides [18].

As was argued above, it is important to understand the W-SiC interaction and thermal stability before making use of W as a coating layer on the TRISO particle. In this work, we focus on investigating the interfacial reactions and surface analysis between thin W films and single-crystalline 6H-SiC polytype substrate at temperatures ranging from 700 °C to 1000 °C. The temperatures range of 700 °C to 1000 °C was used to be able to identify the initial reaction temperature, reaction products and structural changes.

## 2. Experimental Procedure

Semi-insulating 6H-SiC single-crystal wafers, of 2 inch diameter, 330 μm thickness, with a micro pipe density < 10 cm<sup>-2</sup> and root mean square (rms) surface roughness of < 0.5 nm was used as starting material. The 99.9% pure W sputtering target was obtained from AJA International Inc. Thin W films were sputter-deposited on the 6H-SiC wafer by initially mounting the wafer on a rotating sample holder to ensure that a uniform layer was deposited. The base pressure in the chamber was first pumped down to 10<sup>-7</sup> Torr and then subsequently filled with Argon (Ar) gas to a pressure of 10<sup>-3</sup> Torr. The Ar gas flow was kept constant at 8.0 sccm/min. W target (DC sputtering) was sputter-cleaned for 10 minutes using Ar plasma before the actual sputtering process was done at room temperature. A thin-film layer of W was successfully deposited on the SiC substrate and the samples were subsequently annealed in a high vacuum (HV) computer-controlled Webb 77 graphite furnace at temperatures of 700 °C, 800 °C, 900 °C and 1000 °C for 1 hour.

All the samples were analysed using Rutherford backscattering spectrometry (RBS) before and after annealing and simulated using the RUMP code to obtain the thickness of the W deposited layer, composition of deposited layer, check for interdiffusion across the interface and obtain the composition of the reaction zone. The energy of the He<sup>+</sup> ions used was 1.6

MeV, with partially depleted PIPs detector set at a backscattering angle of  $165^\circ$ . The sample was tilted  $4^\circ$  away from the normal, and the solid angle of the detector was 3.41 msr. During the analysis 8  $\mu\text{C}$  of charge was collected, with beam current of 12 nA. The vacuum pump system is composed of the fore pump and turbo pump was used to provide vacuum pressure in the  $10^{-7} - 10^{-8}$  mbar range during analysis which was done in an oil free chamber. XRD analysis was performed using a Bruker D8 Discover XRD system with a Cu  $K_\alpha$  radiation source and the ICDD PDF2 database to identify the phase formation and orientation before and after heat treatment of the samples. A field-emission scanning electron microscopy (FESEM) powered with a Zeiss Ultra 55 high resolution field emission microscope was used to study the surface morphology of the samples before and after annealing at the different temperatures.

### 3. Results and Discussion

#### 3.1. RBS

Typical RBS spectrum of W deposited on 6H-SiC is shown in Fig. 1 and the corresponding simulated spectrum obtained by RUMP [21] computer code is also included. The arrows in

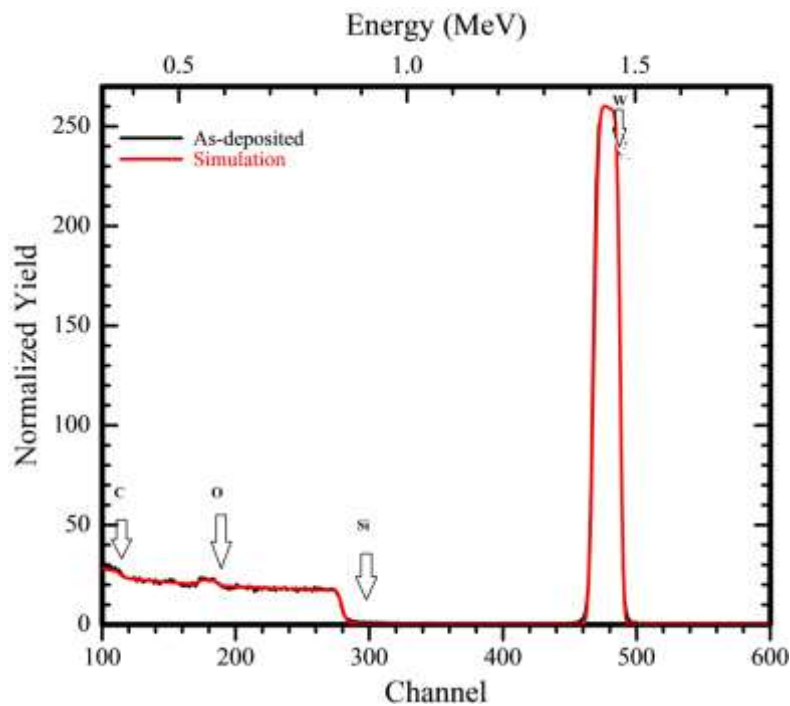


**Fig. 1:** Overlay of the as-deposited RBS spectrum of W deposited on 6H-SiC and the simulated spectrum obtained using RUMP code.

Fig. 1 indicate the surface channel positions of the elements indicated. The thickness of the deposited layer obtained from RUMP simulations was 65 nm and was composed of 63.4 at.% W and 34.4 at.% O. These results indicate that the deposited W layer consisted of some oxide. Oxidation of W might have been occurred during the sputter deposition process.

The RBS spectra of the as-deposited W thin film, after annealing for 1 hour at 700, 850 and 900 °C are depicted in Fig. 2. The RBS spectra of samples annealed at 700 and 800 °C (not shown here) matched the as-deposited spectrum. But closer inspection of the region between channel numbers 200 and 320 (inset in Fig. 2), the spectrum of the sample annealed at 700 °C indicates a slight shift of the Si edge towards lower channels. This implies that diffusion of W into SiC had occurred but no reaction was detected by RBS analysis at these annealing temperatures.

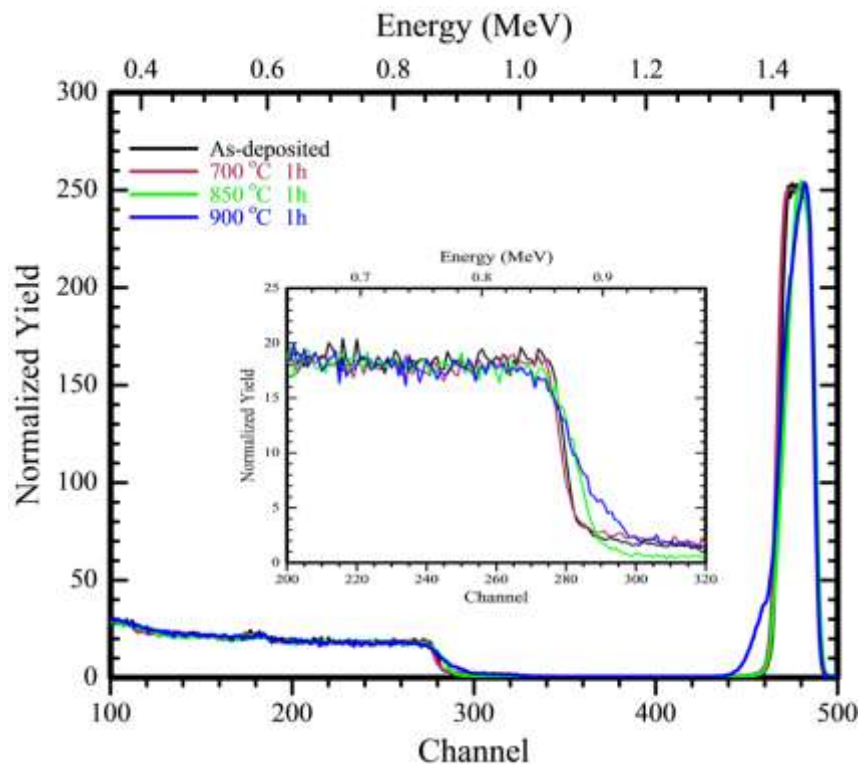


**Fig. 2:** RBS spectra of as-deposited W-SiC sample compared with those annealed 700, 850 and 900 °C for 1 hour and insert of magnified Si signal from channel numbers 200 to 320.

The RBS spectra of samples annealed at 850 °C indicated a reduction in the W peak height at the low energy channels and this was accompanied by a shift of the Si edge to higher energy channels. This observation implied that reactions between W and SiC at the interface began at this temperature. Annealing at 900 °C caused further reduction at the top low energy edge

of the W peak. This resulted in a step appearing at the bottom of the W peak extending towards lower energy channels. Concurrently, further shift of the Si signal towards higher energy channels was also observed after annealing at this temperature. These results indicate that W/SiC interactions took place at the W-SiC interface after annealing at 850 °C, which led to further widening of the interaction region after annealing at 900 °C. No phase formation could be detected from the C peak (superimposed on the Si signal) due to the low sensitivity of RBS to low Z atoms such as C. The peak height of at the surface of the W thin film did not reduce, indicating that there was unreacted W at the surface and only the W at the interface reacted.

### ***3.2. X-ray diffraction***

XRD patterns of W deposited on 6H-SiC after vacuum annealing at temperatures from 700 °C to 1000 °C for 1 hour are shown in Fig. 3, the as-deposited is included for comparison. The as-deposited samples have no distinct XRD peaks except the broad W peaks at 39.2° and 73.2 ° 2 $\theta$  positions. The W broad peaks for the as-deposited might be due to nano-particle size effect or micro-strain. For the samples annealed at 700 °C, a broad diffraction peak corresponding to a 2 $\theta$  value of 39.2° and 73.2° attributed to the (110) and (211) reflection respectively of the W phase were observed. Two new W diffraction peaks appeared at 57.02° and 100.8° 2 $\theta$  positions. The appearance of the new W peaks after annealing at 700 °C indicates that the crystallinity of W thin film had improved. The CW<sub>3</sub> peak attributed to the 44.3° 2 $\theta$  position was present along with WC peaks at 48.5° and 64.2°. This indicated that a reaction responsible for the formation of carbides had occurred at this temperature. In this study, we only observed the formation of carbides from 700 °C. A peak indexed to WO<sub>2</sub> at 36.9° indicating that the W thin film had oxidised.

After annealing at 800 °C, peaks indexed to CW<sub>3</sub> at 44.3° and WC at 48.5° and 64.2° were observed, which were narrower compared to 700 °C patterns. The W tungsten peaks (at 40.3°, 73.4° and 100.8°) increased in intensity and became less broad. These indicated that W was becoming more crystalline. This reaction between C and W at 800 °C was not detected by the RBS analysis because it is highly sensitive to heavy elements as compared to light elements like C.

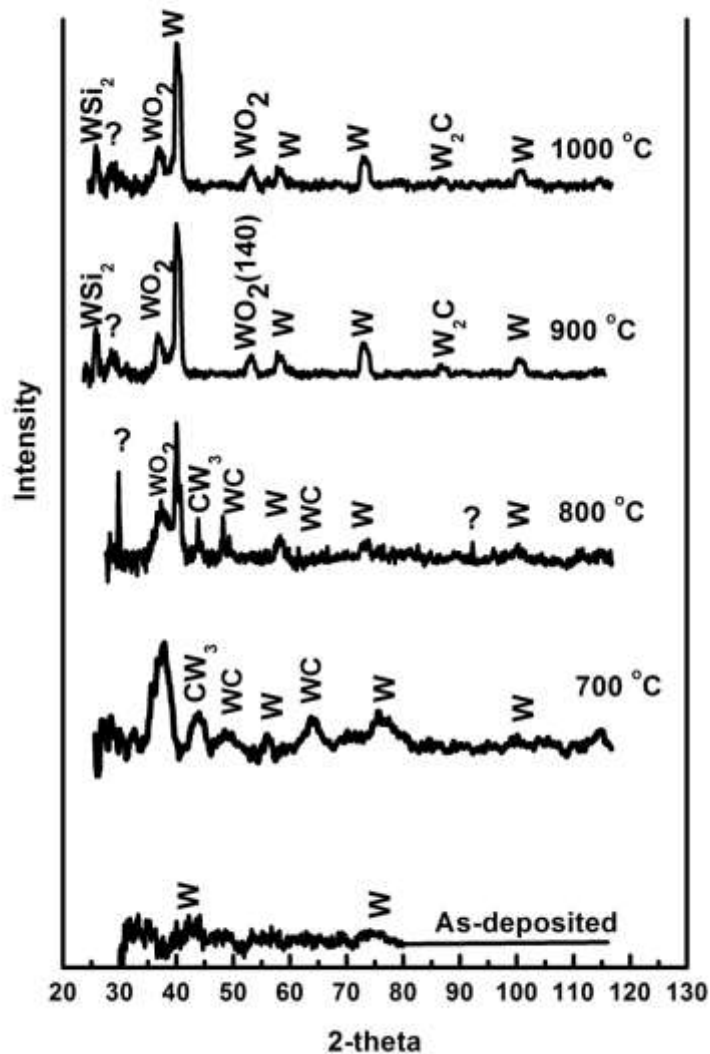


**Fig. 3:** X-ray diffraction patterns of as-deposited W-SiC sample and after annealing at 700 °C, 800 °C, 900 °C and 1000 °C.

After annealing at 900 °C and 1000 °C, a peak indexed to  $\text{WSi}_2$  appeared at  $26.3^\circ$   $2\theta$  position and a  $\text{WO}_2$  peak at around  $54.1^\circ$  was observed. The intensities of W peaks from 700 °C to 1000 °C increased with increasing temperature. The narrowing of the peak width might be due to the change in the nature of W from the polycrystalline state to crystalline state. The WC and  $\text{CW}_3$  peaks disappeared and the  $\text{W}_2\text{C}$  phase was formed at 900 °C and 1000 °C with  $2\theta$  peak position at  $87.5^\circ$ . These results indicate that WC and  $\text{CW}_3$  were not stable at 900 and 1000 °C. Baud *et al.*[13] found that after annealing W thin films on SiC at 950 °C,  $\text{W}_5\text{Si}_3$  and  $\text{W}_2\text{C}$  formed, while Rogowskia *et al.* [16], after annealing W-SiC contacts at 1000 °C only

found silicides present. The formation of  $WSi_2$  has also been observed after annealing W-SiC samples at temperatures above 700 °C [18, 22]. The presence of W peaks at 1000 °C indicates that W layer has not fully reacted with SiC, this is in agreement with RBS results above.

### 3.3. Scanning electron microscopy (SEM)

Fig. 4 shows SEM micrographs of W deposited on 6H-SiC before and after annealing. The SEM micrograph of the as-deposited sample Fig. 4 (a) shows a fairly uniform surface of the W thin film, with very small grains that are evenly distributed.

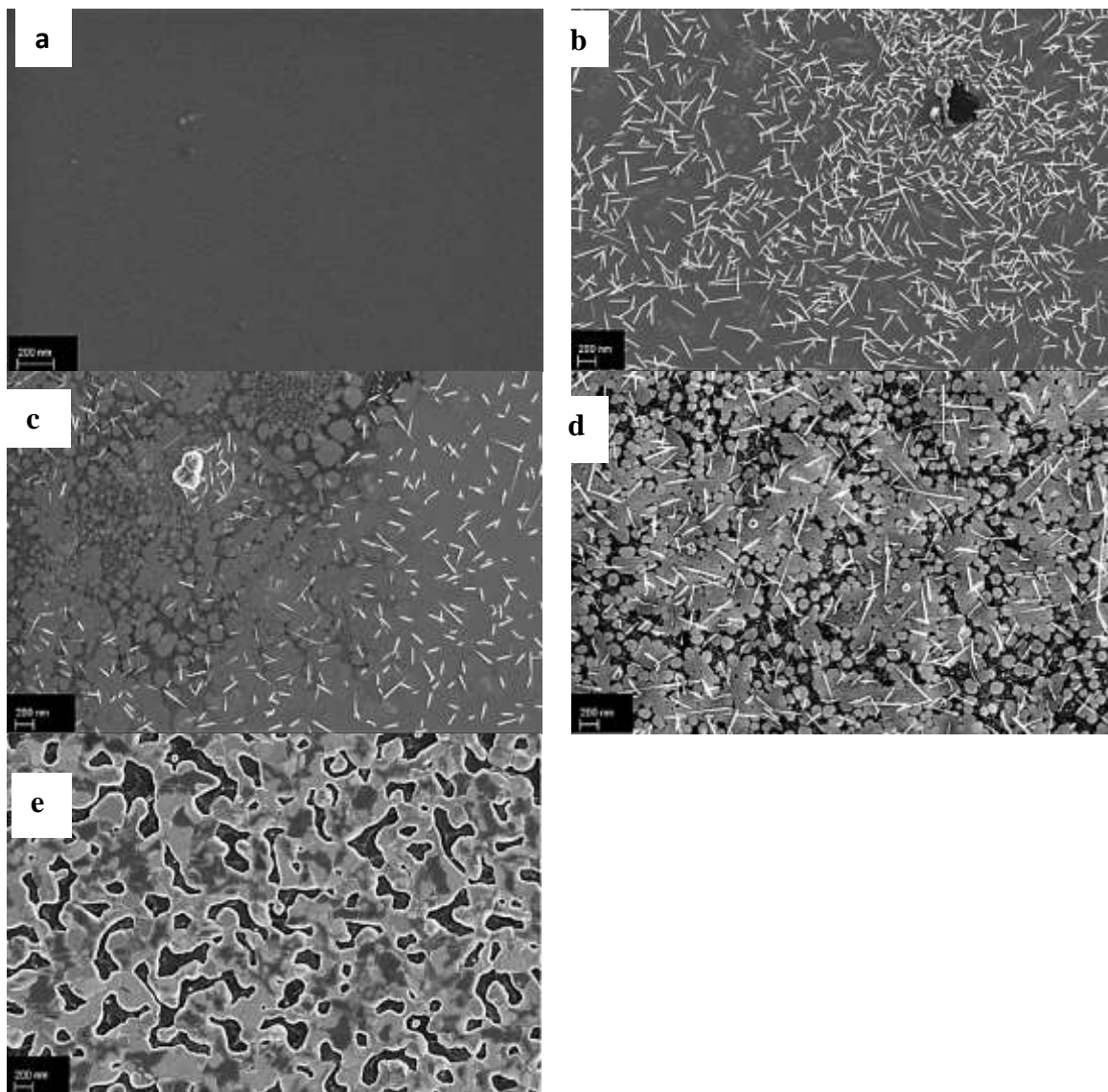


**Fig. 4:** SEM micrographs of W-SiC of (a) as-deposited; vacuum annealed samples for 1 hour at (b) 700 °C, (c) 800 °C, (d) 900 °C and (e) 1000 °C.



The SEM micrograph of samples annealed at 700 °C as shown in Fig. 4 (b) depicts the formation of randomly orientated needle-like crystals covering the surface of W thin film. These needle-like crystals could be WO<sub>2</sub> as identified by the XRD pattern and have been described as “nanowires” by other researchers [23,24]. The SEM micrographs in Fig. 4 indicate that underneath these needle-like structures, agglomeration of the W grains occurred after annealing at 700 °C when compared to the as-deposited sample. There was also a larger range of grain sizes with some varied shapes, including some typical crystallites shapes, i.e. square and rectangular shapes appearing.

The sample annealed at 800 °C indicates formation of W islands as shown in Fig.4 (c). The surface became increasingly rough and uneven grain growth was observed with increase in annealing temperature. The WO<sub>2</sub> needle-like structures were still present after annealing at 800 °C but with a decrease in quantity. For samples annealed at 900 °C depicted in Fig. 4 (d), W thin film was no longer homogenous with island structures increasing on the surface. This island formation might be due to the different phases forming at this temperature as shown in the XRD results above, where W reacted with SiC to form both silicides and carbides.

At 1000 °C, the WO<sub>2</sub> crystals that were observed at lower temperatures were no longer visible. This is a result of the increase in the reaction zone thickness and decrease in the unreacted W layer. A difference in contrast was observed on the surface which confirms the possible formation of silicides carbides or oxides, on the W film surface. These results from the SEM images thereby confirm the suggestion earlier made on the broad W peaks seen from XRD analysis for the nano-particle size effect in the as-deposited samples. Thus, we can rule out the possibility for micro-strain contribution.

The driving force of phase formation solid-state reactions is usually thermodynamic (enthalpy of formation) and/or kinetic factors at the interface. For a reaction between W and SiC to occur, SiC must dissociate to Si and C atoms which react with W at the interface to form silicides and carbides [25]. When SiC is in contact with a metal, the enthalpies of formation for carbides and silicides along with kinetic factors determine if a reaction would occur at high temperature. The Si and C atoms then migrate into the W layer and vice versa, leading to the formation of carbides and silicides at 850 and 900 °C as observed in this study.

The heat of formation for the phases in the W-Si-C system have been reported in ref. [22] and the thermodynamically favoured initial phase to form should be WSi<sub>2</sub>. In this study CW<sub>3</sub> and WC were the initial phases observed to have formed with no silicide forming at the W-SiC

interface at a temperature of 700 °C. Seng and Barnes [22] reported that at temperatures of 700 °C and below  $\text{WSi}_2$  and  $\text{WC}$  to be the stable phases present. The presence of carbides at 700 °C is due to the favourable kinetics during annealing.

It was seen from previous studies that the W films which were deposited on SiC with the thickness above 150 nm resulted in the formation of  $\text{W}_5\text{Si}_3$  as the initial silicide[16][13][26]. W films with thickness less than 100 nm resulted in the formation of  $\text{WSi}_2$  [27]. In our case we deposited W thin film of 65 nm on SiC which resulted in the formation of  $\text{WSi}_2$  silicide. Films deposited with a thin W film (<100 nm) will most likely result in a formation of  $\text{WSi}_2$  as one of the initial silicide to form. As mentioned above,  $\text{WSi}_2$  is thermodynamically expected to be the first silicide to form.

## Summary

The interaction of a thin W layer on SiC was investigated. The resulting solid state reactions, phase composition and surface morphology were analysed using RBS, GIXRD and SEM. The samples were vacuum annealed from 700 to 1000 °C in steps of 100 °C for 1 hour. XRD as-deposited pattern was broad showing that the sample was polycrystalline. The surface of the as-deposited samples analysed with SEM showed fairly uniform W thin film, with very small grains that were evenly distributed. XRD analysis results showed the W peak increasing in intensity and narrowing in width with increase in temperature. The change in the XRD pattern of W could be explained by the SEM images. With increase in temperature, the W grains were observed to increase in grain size agglomerating into islands. Oxygen from as-deposited sample was detected on RBS. It was present in a form of  $\text{WO}_2$  from XRD. The  $\text{WO}_2$  was seen on the surface of the W by SEM analysis in a form of randomly orientated needle-like crystals after heat treatment of the samples.

The W/SiC interface was observed to be stable up to a temperature of 700 °C where reaction between W and SiC started to occur. The initial phases formed were  $\text{WC}$  and  $\text{CW}_3$ . These initial phases disappeared after annealing at 900 °C, with a formation of  $\text{WSi}_2$  and  $\text{W}_2\text{C}$  phases. The initial reaction temperature (700 °C) found in our study differs however from bulk W/SiC reaction temperature (1200 °C). The initial phases on bulk SiC were  $\text{W}_5\text{Si}_3$  and  $\text{WC}$ . In our results we also found  $\text{WC}$  as an initial phase but not  $\text{W}_5\text{Si}_3$ . In addition  $\text{CW}_3$  was observed. At 1000 °C the phases found to be stable were  $\text{WSi}_2$  and  $\text{W}_2\text{C}$ .

#### 4. Acknowledgement

This work is based upon research supported by the National Research Foundation (NRF). Any opinion, findings and conclusions or recommendations expressed in this work are those of the authors and the NRF do not accept any liability with regard thereto. T.T acknowledges the financial support from the NRF Doctorate Innovation Fund for her study

#### 5. REFERENCES

- [1] J.B. Malherbe, *J. Phys. D. Appl. Phys.* 46 (2013) 473001.
- [2] E. Friedland, N.G. van der Berg, J.B. Malherbe, J.J. Hancke, J. Barry, E. Wendler, W. Wesch, *J. Nucl. Mater.* 410 (2011) 24.
- [3] E. Friedland, J.B. Malherbe, N.G. van der Berg, T. Hlatshwayo, A.J. Botha, E. Wendler, W. Wesch, *J. Nucl. Mater.* 389 (2009) 326.
- [4] T.T. Hlatshwayo, J.B. Malherbe, N.G. van der Berg, L.C. Prinsloo, a. J. Botha, E. Wendler, W. Wesch, *Nucl. Instr. Meth. Phys. Res. Sect. B Beam Interact. with Mater. Atoms* 274 (2012) 120.
- [5] T.J. Gerczak, B. Leng, K. Sridharan, J.L.J. Hunter, A.J. Giordani, T.R. Allen, *J. Nucl. Mater.* 461 (2015) 314.
- [6] J.H. O'Connell, J.H. Neethling, *J. Nucl. Mater.* 456 (2015) 436.
- [7] J.H. Neethling, J.H. O'Connell, E.J. Olivier, *Nucl. Eng. Des.* 251 (2012) 230.
- [8] J. Veuillen, T. Nguyen Tan, I. Tsiaoussis, N. Frangis, M. Brunel, R. Gunnella, *Diam. Relat. Mater.* 8 (1999) 352.
- [9] I. Tsiaoussis, N. Frangis, C. Manolikas, T.A. Nguyen Tan, *J. Cryst. Growth* 300 (2007) 368.
- [10] E.G. Njoroge, C.C. Theron, J.B. Malherbe, O.M. Ndwandwe, *Nucl. Instr. Meth. Phys. Res. Sect. B Beam Interact. with Mater. Atoms* 332 (2014) 138.
- [11] D.A. Petti, J. Buongiorno, J.T. Maki, R.R. Hobbins, G.K. Miller, *Nucl. Eng. Des.* 222 (2003) 281.
- [12] S. Son, K. Park, Y. Katoh, A. Kohyama, *J. Nucl. Mater.* 329-333 (2004) 1549.
- [13] L. Baud, C. Jaussaud, R. Madar, C. Bernard, S. Chen, *Mater. Sci. Eng. B* 29 (1995) 126.

- [14] J. Tan, Z. Zhou, M. Zhong, X. Zhu, M. Lei, W. Liu, C. Ge, *Phys. Scr.* T145 (2011) 014055.
- [15] L.L. Snead, T. Nozawa, Y. Katoh, T.S. Byun, S. Kondo, D.A. Petti, *J. Nucl. Mater.* 371 (2007) 329.
- [16] J. Rogowski, A. Kubiak, *Mater. Sci. Eng. B* 191 (2015) 57.
- [17] H. Kishimoto, T. Shibayama, T. Abe, K. Shimoda, S. Kawamura, A. Kohyama, *IOP Conf. Ser. Mater. Sci. Eng.* 18 (2011) 162015.
- [18] F. Goesmann, R. Schmid-Fetzer, *Mater. Sci. Eng. B* 34 (1995) 224.
- [19] D. Lee, H. Park, H. Ryu, S. Jeon, S. Hong, *J. Alloys Compd.* 509 (2011) 9060.
- [20] R.W. Balluffi, J.M. Bkakely, *Thin Solid Films* 25 (1975) 363.
- [21] L.R. Doolittle, *Nucl. Instr. Meth. Phys. Res. Sect. B Beam Interact. with Mater. Atoms* 9 (1985) 344.
- [22] W.F. Seng, P.A. Barnes, *Mater. Sci. Eng. B* 72 (2000) 13.
- [23] G.Y. Chen, V. Stolojan, D.C. Cox, C. Giusca, S.R.P. Silva, in: *Emerg. Technol. 2006 IEEE Conf. On. IEEE, 2006, 2006*, pp. 376–378.
- [24] <http://doc.utwente.nl/94220/1/on-chip.pdf>, "On-chip tungsten oxide nanowires based electrodes for charge injection," 10 May 2015
- [25] T.C. Chou, *J. Vac. Sci. Technol. A Vacuum, Surfaces, Film.* 9 (1991) 1525.
- [26] F. Goesmann, R. Schmid-Fetzer, *Mater. Sci. Eng. B* 46 (1997) 357.
- [27] K.M. Geib, C. Wilson, R.G. Long, C.W. Wilmsen, 80523 (1990) 2796.